

# Current Sensors for Monitoring and Protecting Devices in the Alternating Current Traction Power Network

Amirov S. F.  
Norjigitov S. A.  
Karimov I. A.

Tashkent State Transport University, Tashkent  
Tashkent State Transport University, Tashkent  
Tashkent State Transport University, Tashkent

**General Background:** The reliable operation of AC traction power networks is increasingly critical as electrified railway lines expand. **Specific Background:** Existing monitoring systems in Uzbekistan rely solely on measurements at substations, leaving long contact networks unmonitored and vulnerable to voltage loss and interphase short circuits, especially in neutral sections. **Knowledge Gap:** Current protection methods only respond after an electric arc forms, lacking proactive detection and prevention mechanisms. **Aims:** This study aims to design and test an autonomous current sensor capable of real-time current monitoring and early detection of abnormal conditions to prevent arc formation in neutral sections. **Results:** A functional sensor prototype was developed using a microcontroller-based design that converts catenary current to a unipolar signal, calculates root mean square (RMS) values, and transmits data wirelessly via ESP-NOW. Field tests on an operating traction network demonstrated reliable current measurement but revealed limitations in wireless communication reliability and solar-powered autonomy. **Novelty:** The system integrates low-cost components, high-accuracy analog-to-digital conversion, and autonomous solar power with proactive disconnection capabilities, representing a new approach to early fault prevention in traction networks. **Implications:** With improvements in communication and power supply, the proposed sensor offers a scalable solution for enhancing safety and operational efficiency in modern railway electrification systems.

## Highlights:

- Early detection of interphase short circuits
- Low-cost, autonomous sensor with solar power
- Real-time wireless current monitoring

**Keywords:** Current Sensor, Traction Network, Microcontroller, Wireless Monitoring, AC Railway

---

## Introduction

The construction of the traction power supply system in the Republic of Uzbekistan began in the 1970s, and to this day the architecture of the traction network monitoring system has remained largely unchanged. However, with the increasing length of electrified railway lines, as well as higher requirements for reliability and operational efficiency in maintenance, vulnerabilities in the existing monitoring system are being revealed more frequently. The entire monitoring system of the current traction power supply is based on measuring currents and voltages at traction substations and sectioning posts [1]. On the contact network of interstation sections and stations, there are no devices that provide information about the situation on site. As a result, the traction network dispatcher cannot promptly detect a voltage loss due to wire breakage, a drop in operating voltage caused by load, a change in the direction of power flow in the network, and so on. Under current conditions, effective monitoring of the traction network requires measuring electrical parameters along the entire length of the contact network's feeder zone.

## Theoretical Part

In the field of implementing modern monitoring and automation systems in electrical networks, the scientific works of Kirilenko A.V. [2], Kobets B.B., Volkova I. [3], Bayindir R., Colak I., Fulli G., Demirtas K.O. [4], and Stan M.K. [5] serve as highly valuable resources.

Based on the review of the above-mentioned literature, it has been identified that in modern electrical networks, with the introduction of Smart Grid technology, significant improvements in reliability and operational efficiency of maintenance can be achieved. Moreover, this provides the possibility of monitoring devices along the entire length of power lines.

This technology is based on the collection and processing of data from all points of the network in real time. This task is accomplished through the use of specialized current and voltage sensors.

One of the most vulnerable components of the traction network is the neutral section of the contact line. Interphase short circuits often occur at neutral sections, and in most cases the existing automation and relay protection systems do not respond adequately to prevent such short circuits [6]. The reason for this is the relatively small short-circuit current, which is comparable (600–700 A) to the load currents of electric rolling stock (ERS). To address this problem, researchers such as Figurnov E.P., Bykadorov A.L., Zhukov A.V. [7], Semenova E.Yu., Iodko Yu.I., Karpenko V.I., and Semenova D.V. [8] have developed methods for improving the protection of neutral sections. However, all of these protection methods are activated only after an electric arc has formed between the conductors of the contact suspension within the neutral section. Therefore, it is necessary to develop a method that can disconnect the feeding feeder in advance, thereby preventing the formation of an electric arc.

If the process of interphase short-circuit occurrence at neutral sections is studied in detail, it becomes possible to predict the likelihood of arc formation in advance using a current sensor [9]. For this purpose, the current sensor must periodically measure the current value in the contact suspension, and in the event of exceeding a threshold setting, it should be able to send a message to disconnect the feeding feeder [10].

Based on the stated objectives, a functional block diagram of the current sensor can be developed (Fig. 1). The current sensor is mounted on the catenary messenger wire of the contact suspension [11], [12].

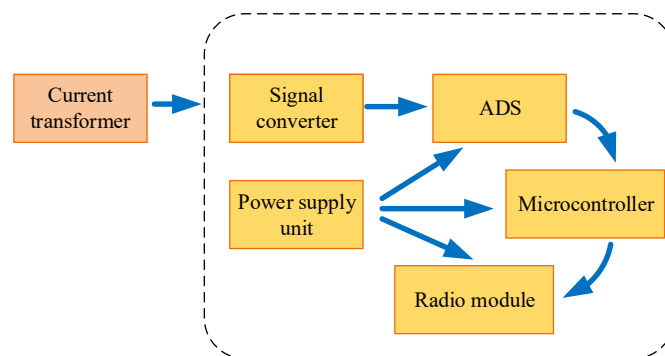


**Figure 1.** Functional block diagram of the current sensor.

A current transformer is installed on the messenger wire, which proportionally reduces the magnitude of the current in the secondary winding. At the same time, it is necessary to take into account the fact that the traction load current is distributed between the contact wire and the messenger wire (if a reinforcing wire is absent) in accordance with the equations [10]:

$$I_{mw} = \frac{Z_{cw}}{Z_{cw} + Z_{mw}} \cdot I_{cn}; \quad (1)$$

$$I_{cw} = \frac{Z_{mw}}{Z_{cw} + Z_{mw}} \cdot I_{cn}. \quad (2)$$

where:  $I_{cn}$ ,  $I_{mw}$ ,  $I_{cw}$  are the currents of the contact network, the messenger wire, and the contact wire, respectively;  $Z_{cw}$ ,  $Z_{mw}$  are the specific impedances of the contact wire and the messenger wire, which are determined by the following formulas:

$$Z_{cw} = r_{cw} + jm \ln \frac{1.28d_{cw}}{R_{cw}}; \quad (3)$$

$$Z_{mw} = r_{mw} + jm \ln \frac{1.28d_{mw}}{R_{mw}}. \quad (4)$$

where  $r_{cw}$ ,  $r_{mw}$  are the specific active resistances of the contact wire and the messenger wire;  $R_{cw}$ ,  $R_{mw}$  are the radius of the wires, and  $d_{cw}$  is the distance between them.

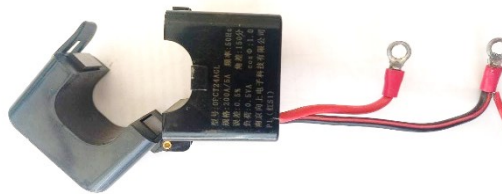


**Figure 2.** Split-core current transformer with a toroidal winding.

As a current transformer, it is possible to use an industrial current transformer with a toroidal secondary winding and a split-core magnetic circuit for ease of installation (Fig. 2). Industrial current transformers are manufactured with a rated secondary current of 5 A.

In order to reduce the impact of inrush currents and short-circuit currents on the analog-to-digital converter (ADC), it is advisable to include a second current transformer in the circuit, as shown in Fig. 3. After repeated transformation, the signal in the form of a sinusoidal voltage must be passed through a low-pass filter (LPF) and converted into a unipolar signal. ADC devices can only process unipolar analog signals.

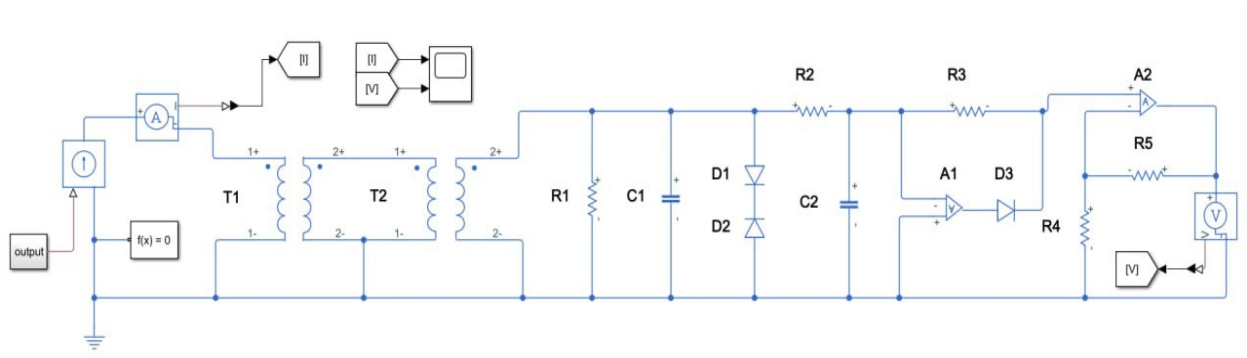


**Figure 3.** Schematic diagram of the current converter block.

Filtering and signal conversion are carried out using operational amplifiers with rail-to-rail characteristics. This approach improves the accuracy of measurement.

To evaluate effectiveness, a mathematical model of the developed circuit was tested in MATLAB Simulink. The oscillograms of the input and output signals are shown in Fig.4. The simulation results were satisfactory: the power of high-frequency noise was reduced, and the signal was successfully converted into a unipolar form.

By using a single potentiometer instead of two resistors (R3 and R4), it is possible to implement signal gain adjustment before feeding it into the ADC.

Signal digitization can be carried out directly in the microcontroller. However, if higher measurement accuracy is required, dedicated ADC modules with higher resolution can be used. For example, the ADS1115 module features a 16-bit ADC capable of measuring input signals with a resolution of up to 0.125 mV. By comparison, most microcontrollers are equipped with a built-in 12-bit ADC, which provides a resolution of about 0.8 mV.

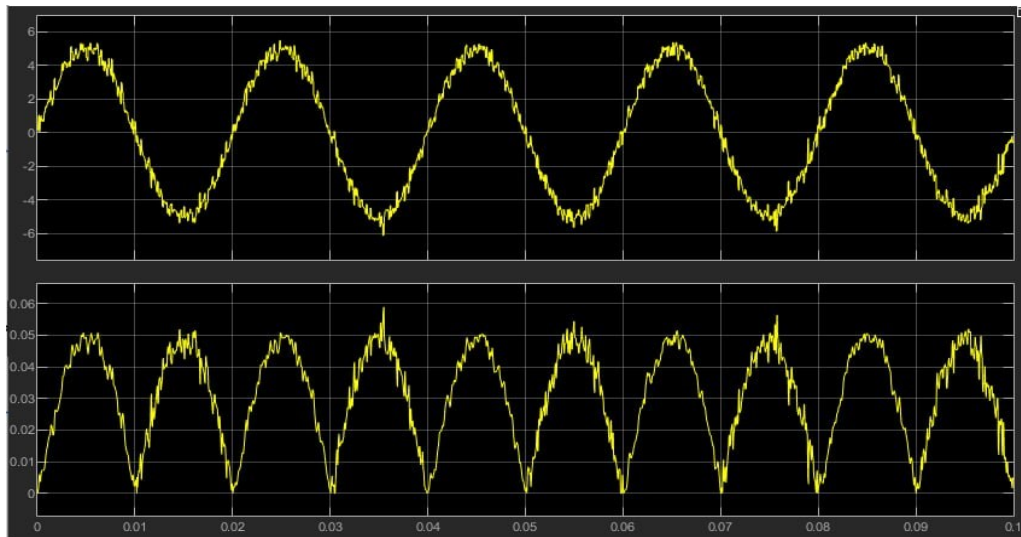


**Figure 4.** Oscillogram of the current converter simulation result.

The data obtained from the ADC are transferred to the microprocessor, where the root mean square (RMS) value of the sinusoidal signal is calculated using the following formula:

$$U = \sqrt{\frac{1}{T} \int_0^T U_m^2 \sin^2(\omega t) dt};$$

where:  $U_m$  - the signal amplitude;  $\omega$  - the angular frequency of the signal;  $T$  - the signal period.

The calculated RMS value is periodically transmitted to a repeater or receiver via a wireless network. For this purpose, wireless communication technologies such as LoRa, Wi-Fi, ZigBee, Bluetooth, etc. can be used. To reduce costs, it is possible to use microcontrollers with built-in radio modules, such as the ESP8266 or ESP32. These microcontrollers are capable of exchanging data using the ESP-NOW technology in peer-to-peer (P2P) mode.

For the full operation of the sensor, it is necessary to provide an autonomous power supply. Autonomous power for the sensor can be implemented using rechargeable batteries and solar panels. The technical characteristics of the batteries and solar panels are selected based on the sensor's energy consumption volume. The daily energy consumption must satisfy the following expression:

$$W > W_{ADC} + W_{MCU} + W_R + W_L.$$

where:  $W$  - the daily amount of energy generated by the source;  $W_{ADC}$ ,  $W_{MCU}$ ,  $W_R$ ,  $W_L$ , are the daily energy consumption of the ADC block, the microcontroller, the radio module, battery recharging, and losses, respectively.

The daily energy consumption of the ADC block, microprocessor, and radio module, as well as the recharging of the batteries, can be calculated on the basis of the technical specifications provided in the device datasheets. The amount of energy loss depends on the resistance and length of the connecting wires between the devices. It is also necessary

to take into account the duration of daylight hours, during which the solar panel powers all devices and has sufficient time to recharge the batteries.

## Sensor Fabrication

The current sensor operates in an environment with very high electromagnetic field exposure. Therefore, with the exception of the main current transformer and the antenna of the radio module, all sensor components must be placed inside a shielding enclosure. Based on this requirement, the protected sensor components are mounted on a single board and placed in a metallic enclosure. After fabrication, the board and the enclosure appear as shown in Figure 5.

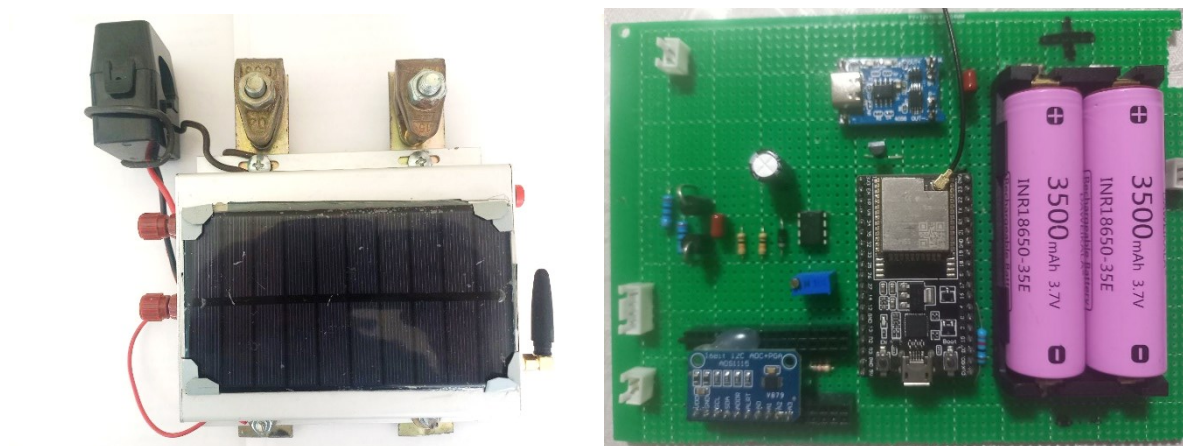


**Figure 5.** External view of the current sensor and the circuit board inside the enclosure.

To process and retransmit the signals received from the sensor, a special module must be fabricated (Fig. 6). This module is installed away from current-carrying parts, in a location convenient for maintenance. The distance between the repeater module and the sensor should not exceed 30 meters, since the quality of the ESP-NOW signal must not deteriorate.



**Figure 6.** External view of the repeater module and the device inside the enclosure.

The ESP32 microcontroller installed in the repeater module receives data from the sensor, compares it with the preset current threshold, records the data on a MicroSD memory card, and visualizes the real-time data on an OLED display. In case the current value exceeds the threshold, a signal to disconnect the feeder circuit breaker is transmitted via the LoRa module. Depending on the terrain conditions, antenna placement, and the power of the transmitted radio signal, the distance between the repeater and the receiver at the circuit breaker may vary within the range of 3–10 km.



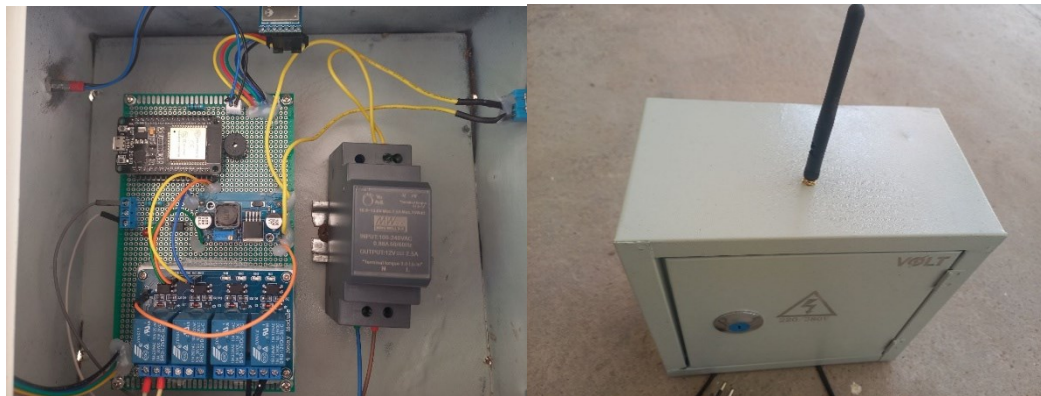


**Figure 7.** External view of the receiver module and the internal layout of the device in the enclosure.

The receiver module is installed in close proximity to the feeder circuit breaker, which is located either at the traction substation or at the sectioning post (Fig. 6). The receiver module is also controlled by a microcontroller, which receives the signal from the radio module and transmits the command to the output relay. After the circuit breaker is tripped, a notification is sent back to the repeater to stop the periodic transmission of trip commands.

To evaluate the effectiveness of the developed system, tests of the sensor, repeater, and receiver were carried out on an active traction power network. The current sensor was mounted on the messenger wire of the catenary system at the Dalaguzar railway station. The repeater module was also attached to the catenary mast near the sensor. The receiver was installed and connected to the backup circuit breaker of the catenary system at the Dalaguzar traction substation. The repeater was configured with a current threshold of 1 A. The test was conducted over a period of 24 hours.

During the testing process, each time the pantograph of the electric rolling stock (ERS) passed under the current sensor, a signal was received from the receiver to trip the circuit breaker. Over the course of 24 hours, the receiver transmitted a trip signal to the circuit breaker 12 times [13], [14].

After the completion of the tests, the data recorded on the MicroSD card were analyzed. The graph of the daily current variation on the messenger wire of the catenary system is shown in Fig. 8. The graph of the daily variation of the sensor's battery charge level is shown in Fig. 9.

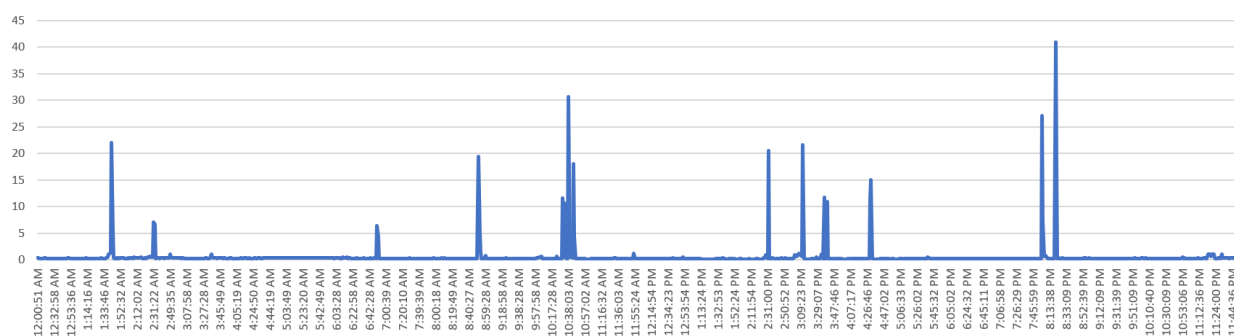


**Figure 8.** Daily variation of current measured by the sensor.

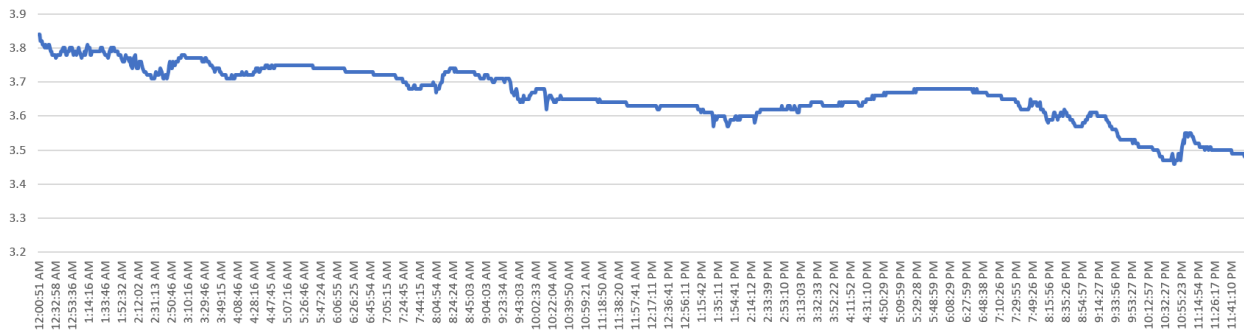


**Figure 9.** Daily variation of the sensor battery charge level.

According to the current graph, during the day the current exceeded the setpoint 14 times, but the receiver received the signal only in 12 cases. This indicates that the radio modules do not ensure reliable signal delivery[15].

The voltage level of the rechargeable batteries decreased from 3.85 V to 3.48 V within a day, which indicates insufficient power of the solar panel.

## Conclusions

Based on the results of the test, the following were determined:

1. With the exception of certain shortcomings, the current sensor and auxiliary modules fulfilled the assigned tasks.
2. The communication method between the repeater and the receiver needs to be revised. It is advisable to use the local wired railway network as the main communication channel, while the wireless method should be used as a backup communication channel.
3. It is necessary to replace the solar panel with a more powerful one. In addition, the microcontroller's program code should be revised to optimize power consumption.
4. After improvements and elimination of the above-mentioned shortcomings, the system must undergo repeated testing.

## References

- [1] V. A. Bykov, V. A. Zimakov, and V. Y. Ovlasyuk, *Electronic Devices of Relay Protection and Automation in Traction Power Supply Systems*. Moscow, Russia: Transport, 1974.
- [2] A. V. Kirilenko, *Intelligent Power Systems: Elements and Modes*. Kyiv, Ukraine: Institute of Electrodynamics of the National Academy of Sciences of Ukraine, 2014.
- [3] B. B. Kobets and I. O. Volkova, *Innovative Development of the Electric Power Industry Based on the Smart Grid Concept*. Moscow, Russia: IAC Energiya, 2010.
- [4] R. Bayindir, I. Colak, G. Fulli, and K. O. Demirtas, "Smart Grid Technologies and Applications," *Renewable and Sustainable Energy Reviews*, vol. 66, pp. 499–516, 2016, doi: 10.1016/j.rser.2016.08.002.
- [5] M. K. Stan, *Smart Grid: Modernizing Electric Power Transmission and Distribution*. The Capitol Net, 2009.
- [6] E. P. Figurnov, *Relay Protection: Textbook for Railway Transport Universities*. Moscow, Russia: Zheldorizdat, 2002.
- [7] E. P. Figurnov, A. L. Bykadorov, and A. V. Zhukov, "Method for Protecting Neutral Sections of AC Contact Networks," *Russian Patent 2241295C2*, 2004.
- [8] E. Yu. Semenova, Yu. I. Iodko, V. I. Karpenko, and D. V. Semenova, "Device for Isolating the Junction of the Contact Network and the Neutral Section for High-Speed Railway Lines Electrified by AC," *Russian Patent 2533768C1*, 2014.
- [9] Z. Tian, N. Zhao, S. Hillmanssen, S. Su, and C. Wen, "Traction Power Substation Load Analysis With Various Train Operating Styles and Substation Fault Modes," *Energies*, vol. 13, no. 11, p. 2788, 2020, doi: 10.3390/en13112788.
- [10] K. G. Markvardt, *Power Supply of Electrified Railways*. Moscow, Russia: Transport, 1982.
- [11] S. Amirov, I. Karimov, and I. Abduazimova, "Application of the Method of Direct Mathematical Modeling to Diamond-Shaped Contact Lines," *E3S Web of Conferences*, vol. 401, p. 02060, 2023, doi: 10.1051/e3sconf/202340102060.

- [12] E. P. Figurnov, Yu. I. Zharkov, and T. E. Petrova, Relay Protection of AC Traction Power Supply Networks: Textbook for Students of Railway Transport Universities. Moscow, Russia: Marshrut, 2006.
- [13] I. Chernykh, Modeling of Electrotechnical Devices in MATLAB, SimPowerSystems, and Simulink. Moscow, Russia: LitRes, 2022.
- [14] OSJD Commission on Infrastructure and Rolling Stock, Procedure for Calculating and Selecting Protection Settings for AC Traction Networks. Warsaw, Poland: OSJD Committee, 2017.
- [15] Protection of Neutral Sections of AC Traction Substations, Electrification and Power Economy (TsNIITEI MPS), Express Information, Issue 4, 1986.